

An Example of Parts Handling and Self-Assembly Using Stable Limit Sets

T.D. Murphey
Electrical and Computer Engineering
University of Colorado
Boulder, CO 80304
murphey@colorado.edu

J. Bernheisel, D. Choi, and K.M. Lynch
Mechanical Engineering
Northwestern University
Evanston, IL 60208
{bernheiseljd,kmlynch}@northwestern.edu

Abstract— Throwing and catching parts, similar to vibratory agitation, promises to be a powerful manipulation technique, but is analytically complicated by equations of motion involving friction and impacts. However, one can show that some simple part manipulators exhibit limit set behavior, where the parts enter a set that is invariant under the mapping that corresponds to the throwing action. We show that by analyzing limit sets directly we can design parts and their environment so that part feeding or assembling naturally emerges from the dynamics. We include experiments validating both these approaches and a discussion of future work.

Index Terms— parts handling, self-assembly, stable limit sets, manipulation, throwing and catching.

I. INTRODUCTION

Traditional approaches to robotic assembly typically focus on the design of the robot itself. This robot then sequentially takes parts and assembles them into some larger, more interesting structure. However, as the number of parts becomes large, this monolithic approach becomes infeasible. Instead, we focus on designing the parts along with their environment in such a way that the desired assembly is an attractor. This can be achieved by appropriate choices of part characteristics (such as shape, density, wettability, friction, charge, chemical, or other properties) and characteristics of the environment in which they move (such as global fixtures, templates, shaped force fields, and energy input in the form of heating or agitation). When this can be done with minimal or no feedback, then the process is called “self-assembly.”

Self-assembling systems come in many different flavors [1], [9], [10] and are receiving increased attention in the robotics and manufacturing communities [7], [8]. Our interest in this paper is in the assembly of rigid parts, mesoscale or larger, under low-degree-of-freedom external forcing of the parts’ support surface. In short, the goal is to literally throw together an assembly: to design the mass properties of the parts and the motions of the parts’ support surface such that there is a single, globally attractive fixed point of the dynamical system — the desired assembly. In these systems, the dominant forces are contact and restitution forces, friction, and gravity. These systems are driven, dissipative, nonlinear dynamical systems, and the detailed dynamics are complex. Both in the present work and in [6] our approach is to exploit qualitative features

of the dynamical system, such as ergodicity or the existence of limit sets, to find controllers that induce the assembly using a small number of motion primitives and simple sensing. However, in contrast to the work in [6] where we used binary feedback to induce assembly, here we pursue completely open-loop assembly.

The problem of throwing together an assembly is challenging, particularly considering that the only “binding” forces between parts are due to local potential wells induced by gravity and complementary part-part or part-environment geometries. Nonetheless, such a system is not completely without precedent. The commercial Sony APOS parts orienting system (Fig. 1) produces a tray of oriented parts by a simple agitation strategy [3]. Parts wash over the vibrating tray, and the tray has part-shaped depressions such that parts that fall into the depressions in the right orientation stay there, and those that fall in the wrong orientation pop back out. These parts continue into a return bin and then are dumped over the tray again. This process continues several times, with no sensing, and the result is a tray of oriented parts (with perhaps a small number of empty depressions). The design problem is to find an appropriate depression shape and vibration profile for the given part. Currently this problem is solved by experimental trial-and-error.

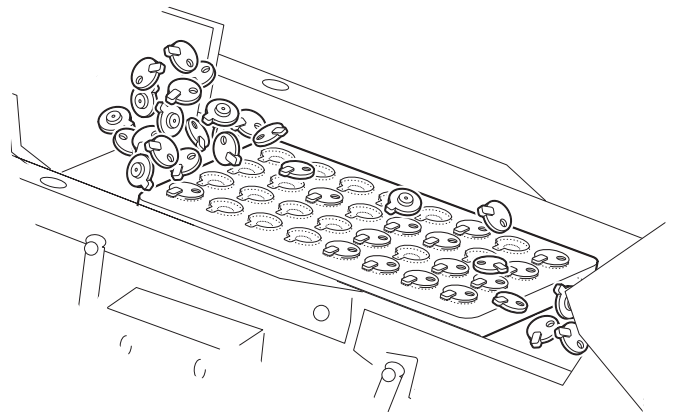


Fig. 1. The Sony APOS parts orienting system (used from [5] with permission).

In this paper we study a very simple system to begin to explore the trade-offs in environment design (fixtures, like the depressions in the APOS tray), environment control variables (agitation), sensing requirements, and part interaction forces (e.g., due to part geometry). Consider the following scenario. Two rigid planar polygonal parts in a gravitational field rest on a support surface. The support surface is a one-degree-of-freedom arm that throws the parts, lets them settle in a new configuration, then throws them again. The goal is to design the throws so that the parts eventually settle in the desired “assembly.” This assembly is at a local minimum in the potential field. This is achieved by designing the limit sets so that parts can only enter a given region of the arm if they are in the proper orientation for assembly. In the present work we achieve this by solving for a combination of part parameters (such as center of mass location) and environment parameters (such as throwing velocity) so that the feeding and assembly behavior naturally occurs.

Although this is a simple toy system, already the dynamics are sufficiently complex, and the control authority sufficiently limited, that the system resists traditional approaches to feedback control design. Instead, we rely on the existence of qualitative features such as limit sets under certain throwing actions. These features can be used to select actions and design simple sensors [2]. Our goal is to understand the minimal set of design, sensing, and control resources, expressed in terms of the environment and the individual parts, that induces the assembly.

The purpose of this paper is to illustrate the potential usefulness of analyzing limit sets as a means of achieving desired behavior such as self-assembly. In this paper, particularly in our choices in modeling, we make many assumptions. We assume that the parts are perfectly rigid as is the arm throwing them, that friction is very high to make the impacts easier to analyze, and that the total energy of the part determines when it will transition between two modes of behavior (as we will discuss in the next section). We additionally assume a small angle approximation holds for purposes of numerical and symbolic computation. All these assumptions allow us to explicitly compute, from first principles, the characteristics of the limit sets as well as explicitly compute root-finding procedures for purposes of mechanical design. The general characteristics of the limit sets are reasonably accurately reflected by these assumptions (as shown in [4]). Therefore, these choices in modeling should be thought of as ways to make the analysis more tractable in the beginning stages of this research. We expect in the future to find that the limit set behavior is relatively robust to changes in mechanical characteristics.

In Section II we review a previous experiment in repetitive throwing and catching of a single part that led to the experiments in this paper. Section III describes the techniques used to design the limit set behavior of a part. Finally, Section IV describes two experiments in self-assembly: controlling a single part to a desired configuration, and controlling two parts to a desired assembly.

II. PREVIOUS WORK

The Flatland testbed for assembling planar parts by throwing and catching is shown in Fig. 2. The Flatland setup is composed of a large air hockey table that can support objects with a nearly frictionless air bearing. The angle of the table is adjustable, providing control on the effect of gravity in the support plane. Parts rest on a 1DOF rotary arm, and we control the motion of the arm to throw the parts. The parts then settle on the stationary arm. The arm is driven by a 1.1 amp Harmonic Drive RH-8 3006 motor. The air table supports an extruded 80/20 aluminum superstructure on which lights and camera are mounted. A Cognachrome vision board calculates the positions of parts on the table for purposes of data acquisition.

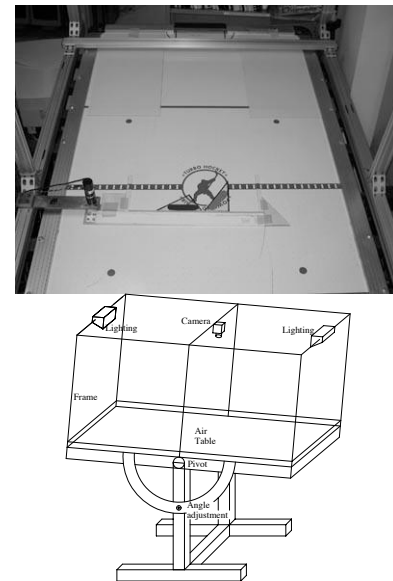


Fig. 2. The Flatland experimental system consists of an “air-hockey” table used as an air-bearing along with a single-degree-of-freedom robotic arm that can throw parts, and a camera used for data acquisition. The goal is to assemble parts on this arm using only the single degree of freedom and no feedback.

An initial experiment by Lynch, Northrop, and Pan [4] studied impulsive throwing and catching of a single polygonal part (Fig. 3). The “throw map” maps an initial configuration of the part to a final configuration after the part settles. The configuration space is $\mathbb{R}^+ \times \mathbb{N} \bmod n$, where $\mathbb{N} \bmod n$ indicates the set of n stable sides the polygon can come to rest on and \mathbb{R}^+ indicates the distance (“radius”) along the arm from the joint. When the arm repetitively executes identical impulsive throwing motions, it was shown that, for some arm geometries and throwing impulses, the part would eventually enter the same limit set of resting configurations regardless of its initial configuration. The cyclic pattern consists of jogs (small translational motions away from the joint while the part remains in the same orientation) and flips (counterclockwise rotation that additionally moves the part back toward the arm joint). A globally attractive forward limit set for a triangular part can be seen in Fig. 4. Label the sides of the triangle

0, 1, 2. The limit set consists of outward jogs on side 0 until the part hits a critical radius at which it flips onto side 1. Then it jogs until it flips to side 2. Finally, it jogs outward to until it flips back to side 0, where the cycle repeats.

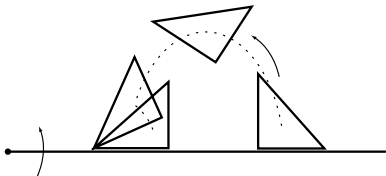


Fig. 3. A part is thrown by an impulse from the rotary arm, then settles back to rest.

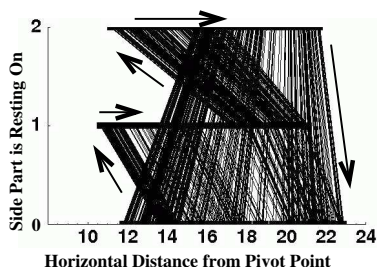


Fig. 4. A simulated limit set for the thrower from Fig. 3. The arrows indicate the motion of the part and its transitions from one side to the next.

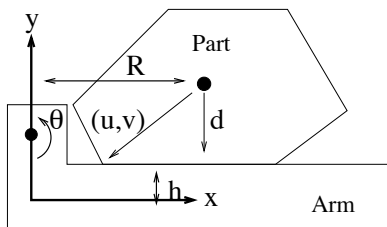


Fig. 5. Part parameters.

To understand this behavior, and to set the stage for our new experiment, we describe the equations of motion for this system. Assume that the part is always thrown such that the left bottom vertex (seen in Fig. 5) always hits the arm first, so that the resulting configuration after a throw will always either be on the initial stable side or on the stable side to the left. Using the parameters from Fig. 5, the (integrated) equations of motion of the part in flight after being thrown at time $t = 0$ are

$$\begin{bmatrix} x(t) \\ y(t) \\ \phi(t) \end{bmatrix} = \begin{bmatrix} R - (h + d^i)\dot{\theta}_r t \\ h + d^i + R\dot{\theta}_r t + \frac{1}{2}gt^2 \\ \dot{\theta}_r t \end{bmatrix} \quad (1)$$

where R is the location of the center of mass of the part on the arm, $\dot{\theta}_r$ is the impulsive angular velocity of the arm, h is the distance from the center of the arm to the edge of the part, and d^i is the distance from the center of mass to the arm when the part is on side i . The x and y coordinates are the location of the center of mass with respect to an inertial frame at the arm's joint and ϕ is the angle of the part with

respect to the arm. (Note that when the arm is horizontal we have $R = x$.) The location of the (initially bottom left) vertex can be written

$$\begin{bmatrix} V_x(t) \\ V_y(t) \end{bmatrix} = \begin{bmatrix} x(t) \\ y(t) \end{bmatrix} + \begin{bmatrix} \cos(\phi(t)) & -\sin(\phi(t)) \\ \sin(\phi(t)) & \cos(\phi(t)) \end{bmatrix} \begin{bmatrix} u \\ v \end{bmatrix} \quad (2)$$

where u, v are the coordinates of the vertex in a body frame at the part's center of mass and aligned with the inertial frame at $t = 0$. Substituting Eq. (2) into Eq. (1) and knowing (by assumption) that the time of impact will be when the left bottom vertex hits the horizontal arm ($V_y(t) = h$), we see that we have to solve

$$h + d^i + R\dot{\theta}_r t + \frac{1}{2}gt^2 + \sin(\dot{\theta}_r t)u + \cos(\dot{\theta}_r t)v = h \quad (3)$$

for the smallest positive value of t , as there may be multiple solutions because of the trigonometric terms. Moreover, we assume that the impulses are sufficiently small and friction is sufficiently high that the left bottom vertex will always be the one that hits the arm and that it will stick after hitting. That is, we do not allow the object to rotate more than one side at a time and we do not allow for chattering after impact. Even with these simplifications, the throw map dynamics cannot be solved analytically.

It was shown in [4] that in this system a part will enter a unique forward limit set for a wide range of initial conditions, given an appropriately chosen $h > 0$ and $\dot{\theta}_r > 0$. That is, if we denote the resting location on the arm by x , the stable side the part is resting on by i , and the throw map from initial condition (x_0, i_0) to final position (x_f, i_f) for a given input $\dot{\theta}_r$ by $T(x_0, i_0)$, the part will enter a set of configurations $S \subseteq \mathbb{R}^+ \times \mathbb{N} \bmod n$ such that $T(x, i) \in S$ for all $(x, i) \in S$. For an approximation of this system it is true that the trajectories will repeat themselves over time [4], because only a finite number of throws are required before a part will flip onto another side and there are only a finite number of sides.

It was shown in [6] that binary feedback is sufficient to both control a part to the end of the arm at a desired orientation and to assemble two parts on the arm. Although the use of some feedback may be required for some applications, our main intent here is to show that self-assembly is possible using only rigid body properties of the parts and no feedback.

III. OPEN LOOP MANIPULATION USING LIMIT SETS

We now address the contribution of this paper—open loop manipulation using the limit sets described before (such as in Fig. 4). Our purpose is to design the limit sets to produce a desired behavior. In this case, we will design the limit sets to guarantee that a part can only reach a particular location on the arm if it is in the desired orientation. We first compute an approximation of the throw map mapping initial conditions (x_0, i_0) to final position (x_f, i_f) . We use this to compute the critical points at which the part will change from “jogs” to “flips.” Then one can use a nonlinear root finding algorithm to solve for physical parameters given desired critical points. The design of the parts handling is therefore completely in terms of the critical points associated with the limit set

behavior. One can choose any number of physical parameters to vary, including density, center of mass location, throwing velocity, side length, etc. We will only vary the center of mass location and the throwing velocity due to the simplicity of experimental implementation, but note that the approach presented here is equally valid for other choices. In fact, all that is required is that the mapping from the parameter space to critical points be onto.

A. Computing the limit set critical points for the thrower

We need to find an analytical set of relationships between a limit set (such as that found in Fig. 4) and the physical parameters we have control over. To this end, define the critical points r_i for each side i as those points such that the throw map $(x_2, j) = T(x_1, i)$ satisfies

$$j = \begin{cases} i & \text{if } x < r_i \\ i + 1 & \text{if } x > r_i \end{cases}$$

We will want to compute r_i for every side i such that for all $R < r_i$ we have a jog and for all $R > r_i$ we have a flip, based on the equations in Eqs. (1-3). The part will flip whenever its post-impact total kinetic energy (including both linear and rotational energy) is greater than the post-impact potential energy as the part rotates around the vertex in contact with the arm. Therefore, we need to find the conditions under which the post-impact kinetic energy is greater than the post-impact potential energy.

Although we can certainly solve Eq. 3 numerically for the post-impact location and energy, our purpose is to find criteria for designing system attributes, such as center of mass location, in order to have desired critical points r_i . However, we cannot analytically solve for energies because of transcendental equations arising due to the sine and cosine terms. Therefore, we make the ‘‘small angle’’ approximation (i.e., we are going to linearize the sine functions around $\dot{\theta}_r t = 0$ because for each throw t is relatively small). This means that we replace $\sin(\dot{\theta}_r t)$ with its linearization $\dot{\theta}_r t$ and $\cos(\dot{\theta}_r t)$ with 1. If we solve

$$V_y(t) = h + d + R\dot{\theta}_r t + \frac{1}{2}gt^2 + \dot{\theta}_r tu + v = h$$

for $t > 0$ (and making g positive), we get

$$t = \frac{2\dot{\theta}_r(R + u) + \sqrt{4\dot{\theta}_r^2(R + u)^2 - 8g(d + v)}}{2g}.$$

Setting $d = -v$, we get

$$t = -\frac{2\dot{\theta}_r(R + u)}{g}.$$

Plugging this into Eq. (1) we get new coordinates $[x(t_{\text{impact}}), y(t_{\text{impact}}), \phi(t_{\text{impact}})] =$

$$\begin{bmatrix} R + \frac{1}{g}2\dot{\theta}_r(R\dot{\theta}_r + \dot{\theta}_r u)(h - v) \\ -\frac{1}{g}2R\dot{\theta}_r(R\dot{\theta}_r + \dot{\theta}_r u) + \frac{1}{g}2(R\dot{\theta}_r + \dot{\theta}_r u)^2 - v \\ -\frac{1}{g}2\dot{\theta}_r(R\dot{\theta}_r + \dot{\theta}_r u) \end{bmatrix}.$$

Let $[r_x, r_y]$ be the vector from the center of mass to the vertex that impacts the arm. Moreover, let m denote the mass of the part and ρ denote the radius of gyration of the part. Then, under the assumption that the impacting vertex does not slide, the pre-impact and post-impact velocities are related by

$$\dot{x}^+ - r_y\dot{\phi}^+ = 0 \quad (4)$$

$$\dot{y}^+ - r_x\dot{\phi}^+ = 0 \quad (5)$$

$$r_x(\dot{y}^+ - \dot{y}^-) - r_y(\dot{x}^+ - \dot{x}^-) = \rho^2(\dot{\phi}^+ - \dot{\phi}^-) \quad (6)$$

(see [4] for details). Now solve for $\dot{\phi}$ after impact using Eqs. (4-6) and get

$$\dot{\phi}_{\text{new}} = -\left(\frac{-\rho^2\dot{\theta}_r + u(R\dot{\theta}_r - 2(R\dot{\theta}_r + \dot{\theta}_r u)) - \dot{\theta}_r v(-h + v)}{\rho^2 + u^2 + v^2}\right)\dot{\theta}_r.$$

With this we can determine the kinetic energy after impact,

$$K = \frac{\rho + m(u^2 + v^2)}{2(\rho^2 + u^2 + v^2)^2} \left(-\rho^2\dot{\theta}_r + u(R\dot{\theta}_r - 2(R\dot{\theta}_r + \dot{\theta}_r u)) - \dot{\theta}_r v(-h + v) \right)^2.$$

Moreover, the potential energy after impact is:

$$V = -gm \left(\frac{1}{g}2R\dot{\theta}_r(R\dot{\theta}_r + \dot{\theta}_r u) - 2(R\dot{\theta}_r + \dot{\theta}_r u)^2 + v + \sqrt{u^2 + v^2} \right).$$

Hence, we now have, for every side i , a function $F = K - V$ that is zero precisely when the part transitions from jogs to a flip. Zeros of this function therefore determine the critical points of the limit sets. Note that the function F depends on both physical parameters (in this case $(u, v, \dot{\theta}_r)$) and the location on the arm R .

We now consider whether or not the function $F = K - V = 0$ is locally solvable for $(u, v, \dot{\theta}_r)$ given a set of desired critical points r_0, r_1, r_2 . For instance, consider a triangle like the one pictured in Fig. 3 with the center of mass at $(u, v) = (2, 3.5)$ with respect to the hypotenuse. Figure 6(a) shows the corresponding limit set with $\dot{\theta}_r = 320$. It is clear that one cannot predict the orientation of a part purely by its location on the arm. Instead, we would like a limit set that is skewed so that some areas on the arm can only be reached in a particular orientation. The determinant of the Jacobian of the function F is nonzero near the operating point $(u, v, \dot{\theta}_r) = (2, 3.5, 320)$, so we can locally deform the limit set. If we choose a new limit set of $(r_0, r_1, r_2) = (10, 10, 20)$, we find (using the *Mathematica* **FindRoot** command) that a choice of $(u, v, \dot{\theta}_r) = (2.8, 3.8, 263)$ gives rise to these critical points. Figure 6(b) shows an intermediate calculation in this root finding process and Fig. 6(c) the final limit set. This last limit set is more desirable because we know (by inspection of the limit set) that if the part’s x position is greater than 20 inches, the part must be on side 2. Hence, if we convey or trap the part at that location, it will be in a known configuration. Moreover, if we have two parts that we would like to assemble, we can use this limit set behavior to assemble them, provided we ignore inter-part effects (which may not be negligible). We will discuss experimental implementations of both these ideas in Section IV.

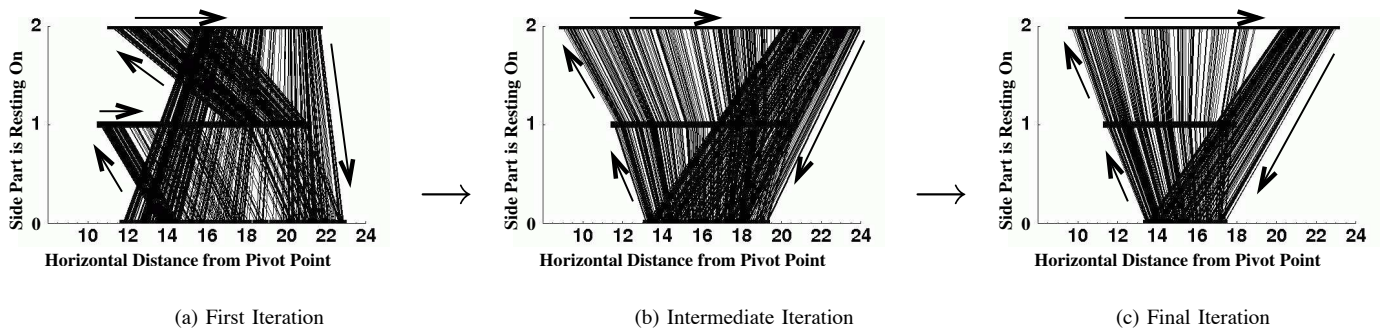


Fig. 6. A sequence of iterations in the numerical root-finding techniques used to determine the part shape. The first initial shape has the part reaching the same location on the robotic arm for each side. That is, the part flips to a new side by the time it reaches 20 cm, regardless of what side it is on. By changing the physical parameters (in this case the center-of-mass) one is able to compute a part that will only go to the end of the arm if it is on side 2. Hence, the part has been designed to be “self-assembled” mechanically.

IV. OPEN LOOP EXPERIMENTS

Our implementation of the thrower on the Flatland experiment shown in Fig.2 consists of a servo motor (described earlier) attached to a 0.25" thick piece of plexiglass that rests on the air bearing. The plexiglass is basically rigid as is its connection to the motor. We use the motor to approximate impulses on the part, and the arm is covered in a thin layer of high-friction slow-recovery foam (Lendell Mfg, type PHS-14) to approximate the friction assumptions in the impact analysis.

To implement these ideas experimentally, we started with a right triangle (also made of plexiglass) with side lengths 3.6 – 5.75 – 6.75 (in inches). We then attached a lead weight to the triangle, allowing us to move the center of mass. Numerically, we found that moving the lead weight into one of the corners helped to extremize the limit set, so that r_0 and r_1 are small and r_2 is large. When the part is on its long side (side 2), the part will jog off the arm into a cavity (shown in Fig. 7(b)) that is deep enough that the throws do not have enough energy to eject the part. On sides 0 and 1, however, the part does not reach the cavity. This experiment was repeated 20 times with random initial conditions and was successful 95% of those times (19/20). The one experiment failed because the part hit the wall of the cavity. There is a tendency for this to occur when the center of mass of the part is very close to the end of the arm before the part falls into the cavity. This indicates the need for a better design of the cavity.

For open-loop assembly we design the stable limit sets independently such that both parts only enter the cavity in a desirable configuration. For the first part, we use the same triangle discussed above. For the second, we choose a four-sided polygon that, when placed in the cavity, will perfectly match with the sides of the cavity and the top of the triangle. This is what we consider our “assembled” state. If the limit set of the second part is designed correctly, the two parts will fall into the cavity in the assembled state (Fig. 8).¹

¹For a movie of this experiment as well as the other experiments, please see <http://ece.colorado.edu/~murphey>.

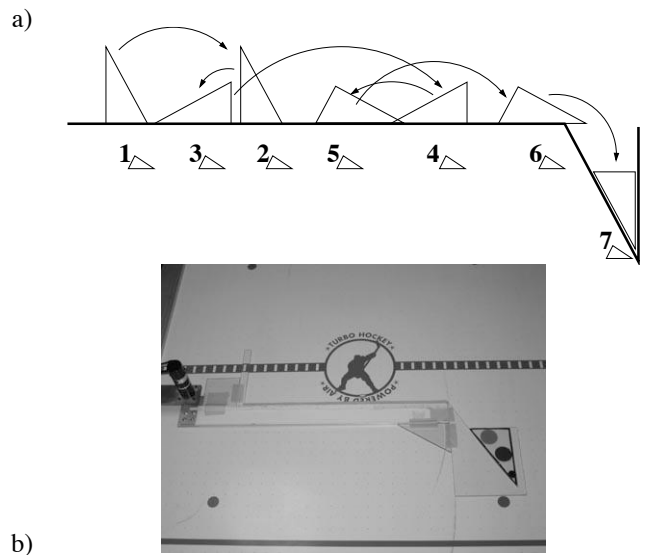


Fig. 7. By designing the limit set for one three sided part, the part is “fed” at a unique orientation off the end of the arm in a completely sensorless fashion. The illustration shows the progress of a triangular part as it is thrown on the arm. (This illustration is for conceptual purposes only. In many cases, more than six throws are necessary for the triangle to reach the end of the arm. In particular, there are typically several jogs in between flips.)

We do not address the difficulty of inter-part interactions and balancing between the extremes of very low energy throws that do not provide stable limit cycle behavior and high energy throws that eject the parts from the cavity. This experiment was repeated 20 times with random initial conditions and was successful only 55% of those times (11/20). Two of the most common failure modes included the second part being ejected from the assembled state on the next throw and the second part becoming stuck in the cavity in an incorrect orientation. These failures are due to two main factors. First, we did not analyze inter-part interaction, which will be a topic of further study. This could be mitigated by having the parts handled separately (either serially or in parallel by two different manipulators) in the experimental implementation. Secondly, we did not analytically design the cavity for capturing the

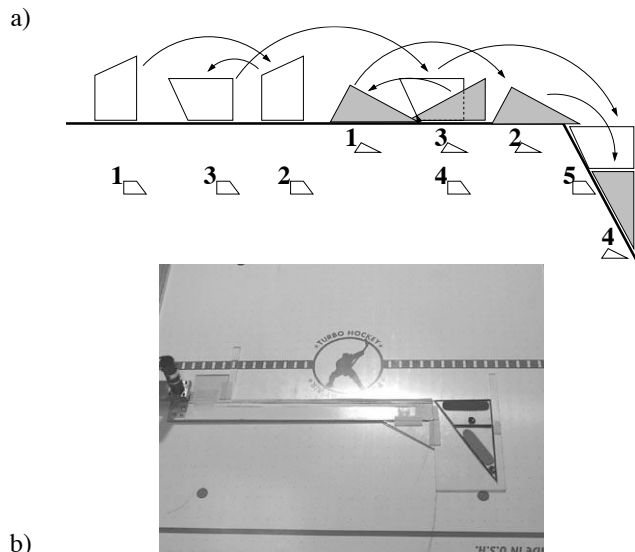


Fig. 8. By designing the limit sets for two parts (one three sided and one four sided), two parts are also “self-assembled” in a completely sensorless fashion. The illustration shows the progress of both parts as they are thrown on the arm and eventually self-assemble at the end of the arm.

parts, which meant that sometimes the parts were ejected before they were successfully assembled. Indeed, once the parts were in their assembled state, the parts only remained assembled after the next throw 85% (17/20) of the time. We anticipate being able to improve these results with more experimentation and analysis.

V. CONCLUSIONS

In this paper we proposed a technique for part manipulation and assembly that relies on the limit set behavior that parts experience during repeated throws. In order to successfully analyze an example system, we made many assumptions in the physical modeling and in the numerical techniques we employed, but we found that these assumptions successfully predicted our ability to design the limit set behavior in the part. This suggests that the limit set behavior is quite robust with respect to the specifics of materials used and other experimental particulars. Hence, we hope that these techniques may be extended beyond their current preliminary stage to develop self-assembly design techniques for a broader class of systems.

For parts sorting and feeding, the proposed approach seems to work very well, and experiments matched analytical predictions quite well. For assembly, more work must be done. The fact that the open-loop assembly worked at all experimentally when only using rigid body properties of the parts and arm indicates the strength of these techniques. However, the fact that it only works a little more than half of the time indicates the need to have better models of inter-part impacts and to design the trapping mechanism. Moreover, the ultimate goal of this research is to be able to successfully self-assemble hundreds of parts, again indicating that inter-part interaction must be a fundamental aspect of further study. This will mean that the explicit integration of the equations of motion (such as that done in Section III-A) will be impossible, leading to the need for implicit techniques that only depend on analyzing the nonsmooth equations of motion for the parts. This will be the object of future study.

ACKNOWLEDGMENT

This work was supported in part by National Science Foundation grants IIS-0082957 and IIS-9811571.

REFERENCES

- [1] N. Bowden, A. Terfort, J. Carbeck, and G. M. Whitesides. Self-assembly of mesoscale objects into ordered two-dimensional arrays. *Science*, 276(5310):233–235, April 1997.
- [2] M. A. Erdmann. Understanding action and sensing by designing action-based sensors. *International Journal of Robotics Research*, 14(5):483–509, October 1995.
- [3] H. Hitakawa. Advanced part orientation system has wide application. *Assembly Automation*, 8(3):147–150, 1988.
- [4] K. M. Lynch, M. Northrop, and P. Pan. Stable limit sets in a dynamic parts feeder. *IEEE Transactions on Robotics and Automation*, 18(4):608–615, 2002.
- [5] M. T. Mason. *Mechanics of Robotic Manipulation*. MIT Press, 2001.
- [6] T. D. Murphey, D. Choi, J. Bernheisel, and K. M. Lynch. Experiments in the use of stable limit sets for parts handling. In *International Conference on MEMS, NANO, and Smart Systems (ICMENS)*, pages 218–224, Banff, Canada, 2004.
- [7] K. Saitou. Conformational switching in self-assembling mechanical systems. *IEEE Tran. on Robotics and Automation*, 15(3):510–520, June 1999.
- [8] K. Saitou and M. J. Jakiela. Subassembly generation via mechanical conformational switches. *Artif. Life*, 2(4):377–416, 1995.
- [9] A. Terfort and G. M. Whitesides. Self-assembly of an operating electrical circuit based on shape complementarity and the hydrophobic effect. *Adv. Mater.*, 10(6):470–473, 1998.
- [10] G. Whitesides and B. Grzybowski. Self-assembly at all scales. *Science*, 295(5564):2418–2421, 2002.